Electrochemistry Communications 120 (2020) 106828

Contents lists available at ScienceDirect

Electrochemistry Communications

journal homepage: www.elsevier.com/locate/elecom

Recent advances on metal nitride materials as emerging electrochemical sensors: A mini review

Saiful Arifin Shafiee[a,b,*], Samuel C. Perry[c], Hairul Hisham Hamzah[d], Mohd Muzamir Mahat[e], Firas A. Al-lolage[f], Muhammad Zahir Ramli[a,g]

[a] Kulliyyah of Science, International Islamic University Malaysia, Jalan Sultan Ahmad Shah, Bandar Indera Mahkota, 25200 Kuantan, Pahang, Malaysia
[b] Occupational Safety and Health Unit, International Islamic University Malaysia, Jalan Sultan Ahmad Shah, Bandar Indera Mahkota, 25200 Kuantan, Pahang, Malaysia
[c] Faculty of Engineering and Physical Sciences, University of Southampton, University Road, Southampton SO17 1BJ, UK
[d] School of Chemical Sciences, Universiti Sains Malaysia, 11800 USM Penang, Malaysia
[e] Faculty of Applied Sciences, Universiti Teknologi MARA, 40450 Shah Alam, Selangor, Malaysia
[f] Department of Chemistry, College of Science, University of Mosul, Mosul 41002, Iraq
[g] Institute of Oceanography and Maritime Studies, Kulliyyah of Science, International Islamic University Malaysia, Kg. Cherok Paloh, 26160 Kuantan, Pahang, Malaysia

ARTICLE INFO

Keywords:
Molybdenum nitride
Zirconium nitride
Nickel cobalt nitride
Glucose sensor
Hydrogen peroxide sensor
And oxygen reduction reaction

ABSTRACT

Metal nitride materials are garnering interest in many fields including electrochemistry, although they are still at an early stage of investigation and underexplored. This mini review provides insights on the latest advancements in the field of electroanalytical chemistry based on metal nitride materials, specifically focusing on the best performing transition metal nitride sensors published between 2017 and 2020 for important targets such as glucose, hydrogen peroxide and dissolved oxygen. Nickel cobalt nitride electrodes demonstrate electrocatalytic behaviours toward glucose oxidation and hydrogen peroxide reduction processes. Meanwhile, zirconium nitride electrodes could replace platinum/carbon electrodes for oxygen reduction reaction. This article also introduces solid molybdenum nitride microdisk electrodes, which can easily be prepared and maintained and show diffusion-control voltammetric responses for the complex peroxodisulfate reduction reaction. This mini review will benefit researchers who would like to delve into the potential of metal nitride electrodes as electrochemical sensors.

1. Introduction

Metal nitride materials gaining increased research attention, as indicated by the growing number of publications with the keyword 'metal nitride' over the past decade reported by Web of Knowledge, refer to Fig. 1. In particular, transition metal nitride materials are of interest mainly because they have high biocompatibility, electrical conductivity, chemical and thermal stability, and resemblance to precious metals in terms of their electronic structure [1–4]. Metal nitride materials have been studied as supercapacitors, batteries, electrocatalysts, and photocatalysts [5–8]. In 2018, Rasaki et al. [9] superficially reviewed several metal nitride and carbide materials mostly for various electrochemical applications. Apart from metal nitride, carbon nitride materials have been studied extensively for electrochemical purposes. Chen and Song [10], Wang et al. [11], Magesa et al. [12], and Xavier et al. [13] recently published comprehensive reviews on carbon nitride electrosensors, so this mini review will not cover carbon nitride electrodes. Herein, a number of transition metal nitride materials, specifically those that are developed for the purpose of chemical detection, are reviewed in depth. This article is divided into two parts, i) nitrided metals that exhibit the best electrocatalytic behaviour for several important reactions and ii) the advancement of metal nitride electrodes.

2. Studies on several popular redox processes using metal nitride electrodes

2.1. Non-enzymatic glucose sensors

In 2018, Hwang and colleagues [14] published a review paper regarding a vast array of electrochemical direct glucose sensors, including Fe_2Ni_2N, Fe_3N-Co_2N, Co_3N, Ni_3N, and Cu_3N. The authors compared the values for the sensitivity, selectivity, stability, repeatability,

* Corresponding author at: Kulliyyah of Science, International Islamic University Malaysia, Jalan Sultan Ahmad Shah, Bandar Indera Mahkota, 25200 Kuantan, Pahang, Malaysia.
E-mail address: sabs@iium.edu.my (S.A. Shafiee).

https://doi.org/10.1016/j.elecom.2020.106828
Received 20 May 2020; Received in revised form 21 August 2020; Accepted 25 August 2020
Available online 31 August 2020

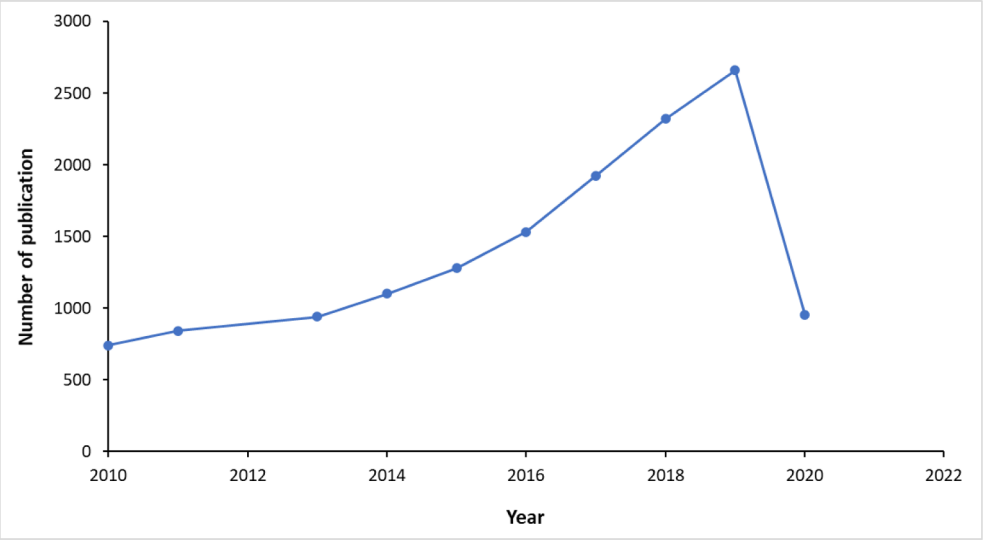

Fig. 1. Number of articles with the word 'metal nitride' as the keyword which have been published over the past decade.

reproducibility, limit of detection, and linear range of the electrodes for glucose oxidation, but did not consider the onset potentials of the redox reaction. Dhara and co-workers [15] reviewed $Co_2N_{0.67}$ and Co_3N as non-enzymatic glucose sensors. The authors compared the values for the sensitivity, limit of detection, linear range, and the peak potential for glucose oxidation, although discussions only covered these two materials. For this article, the onset potentials obtained using various metal nitride electrodes for glucose oxidation were compared to select an electrode material that exhibits the highest electrocatalytic activity towards this redox reaction; this indicates that less overpotential is needed to drive the electrochemical process. All potentials were converted to the scale of Ag/AgCl reference electrode (saturated KCl) for easier comparison. We also compared the values for the sensitivity, limit of detection, and linear range of the electrodes for glucose oxidation to choose the best electrochemical sensor for this electrochemical reaction.

Based on a comprehensive literature search, nickel cobalt nitride ($NiCo_2N$) in the form of core shell nanohybrid modified on nitrogen (N)-doped graphene electrodes demonstrates the highest electrocatalytic activity towards glucose oxidation [16]. To fabricate the electrode, $Ni(NO_3)_2{\cdot}6H_2O$, $Co(NO_3)_2{\cdot}6H_2O$, and NH_2CN were added into a solution of graphene oxide whilst stirring overnight at 80 °C. Then, the mixture was freeze-dried at −50 °C to give a grey powder. The powder was ground and annealed in two steps, which includes polymerisation at around 450 °C. The powder was then heated at approximately 800 °C in a nitrogen atmosphere for 2 h. These heat treatment processes are usually performed to modify the properties of materials of interest [17]. Weakly bounded metal nitride and metal oxide materials were removed from the powder by treating it with 1 M H_2SO_4 at around 80 °C overnight. The treated powder was then washed with ethanol and water repeatedly before being dried at ~60 °C for overnight in a vacuum oven.

The foot of the glucose oxidation wave recorded using $NiCo_2N$ core electrodes starts at approximately 0.2 V *vs*. Ag/AgCl, see Fig. 2 [16]. This is important to ensure that the electrochemical sensor has high selectivity towards glucose; more positive potentials (> 0.7 V *vs.* Ag/AgCl) drive the oxidation of other electroactive species that are found in blood samples, such as L-ascorbic acid, uric acid, and dopamine hydrochloride, which would interfere with the electrochemical results [16]. Deepalaskhmi et al. [16] reported that the sensitivity and the limit of detection of their electrodes toward glucose oxidation are 1803 μA mM^{-1} cm^{-2} and 50 nM (signal-to-noise ratio; S/N = 3) respectively. Their electrodes also offer a wide linear range between 2.008 μM and 7.15 mM.

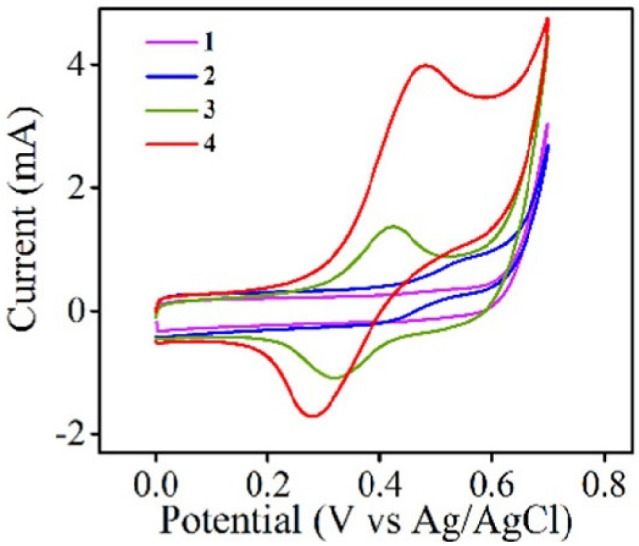

Fig. 2. Cyclic voltammograms recorded using a N-doped graphene/glassy carbon electrode (curve 1 and 2) and a nickel cobalt nitride/N-doped graphene/glassy carbon electrode (curve 3 and 4) in 0.1 M NaOH with the absence (curve 1 and 3) and in the presence (curve 2 and 4) of 1 mM glucose with at 50 mV s^{-1}. This graph was taken from [16] with permission from ACS Publications.

Other metal nitride electrodes, such as nickel nitride (Ni_3N) in different forms [18,19], offer a higher sensitivity for glucose detection than the $NiCo_2N$ electrodes. However, the onset potentials obtained using the other electrodes are more positive than that acquired by the $NiCo_2N$ electrodes. This means that a greater driving force is needed for glucose oxidation to proceed when employing those electrodes compared to when utilising $NiCo_2N$ electrodes.

Deepalakshmi et al. provided insights into the electrochemical behaviour of $NiCO_2N$ electrodes using cyclic voltammetry (Fig. 2). A couple of redox peaks can be seen at around 0.3 V and 0.4 V *vs.* Ag/AgCl in alkaline NaOH solutions even in the absence of glucose, which are attributed to $Ni^{2+/3+}$ and $Co^{2+/3+}$ redox processes occurring within the $NiCo_2N$/N-doped graphene hybrid electrodes [16]. These surface reactions are thought to be key for the glucose oxidation where, Ni^{2+} and Co^{2+} are initially oxidised to Ni^{3+} and Co^{3+}. Glucose is

Table 1
A comparison between the voltammetric features for glucose oxidation obtained using $NiCo_2N$/N-doped graphene nanocore hybrid electrodes, Ni_3N/N-doped carbon microspheres, and Ni_3N nanosheet in 0.1 M NaOH solutions.

Electrode material	Onset/V *vs.* Ag/AgCl	Peak/V *vs.* Ag/AgCl	Scan rate/mV s^{-1}	Linear range/μM	Limit of detection/μM	Sensitivity/μA mM^{-1} cm^{-2}	Ref.
$NiCo_2N$/N-doped graphene	0.2	0.45	50	2–7150	0.05	1803	[16]
Ni_3N N-doped C spheres	0.51	0.63	50	1–3000	0.1	2024.1	[18]
				3000–7000	0.35	1256.9	
Ni_3N nanosheets	0.37	0.57	30	0.2–1500	0.06	7688	[19]

converted to gluconolactone by the oxidised metal sites, which are reduced back to Ni^{2+} and Co^{2+}.

Dai et al. [20] reported the electrocatalytic activity of Ni_3N-Co_3N nanowires on titanium electrodes towards glucose oxidation. They also observed a pair of redox peaks on their cyclic voltammograms at around 0.46 and 0.28 V *vs.* Hg/HgO in the absence of glucose. From the X-ray photoelectron spectroscopy (XPS) analysis, they suggested an alternative mechanism, where Ni^{2+} is oxidised to Ni^{3+} and Co^{2+} is oxidised first to Co^{3+} then further to Co^{4+}. The highly oxidised Ni^{3+} and Co^{4+} are then responsible for oxidising glucose to gluconolactone, returning the metal sites back to Ni^{2+} and Co^{3+} respectively. Deepalakshmi and co-workers [16] should conduct the same analysis to confirm their proposed mechanism.

Insights into key reaction intermediates at $NiCo_2N$ surfaces can be inferred from XPS investigations at related nickel-metal nitrides, such as NiMoN or NiFeN. Reactions at these catalytic metal nitrides begin with the formation of metal hydroxide at the catalyst surface. The route to glucose oxidation can then be expressed in terms of a charge transfer from the electrode to catalytic sites to form the corresponding oxy (hydroxide), followed by a subsequent oxidation of glucose to gluconolactone, as shown in Reactions 1–3 [21].

$$Ni^{2+} + 2OH^- \rightleftharpoons Ni^{II}(OH)_2 \quad \text{(Reaction 1)}$$

$$Ni^{II}(OH)_2 + OH^- \rightleftharpoons Ni^{III}O(OH) + e^- + H_2O \quad \text{(Reaction 2)}$$

$$2Ni^{III}O(OH) + \text{glucose} \rightarrow 2Ni^{II}(OH)_2 + \text{gluconolactone} \quad \text{(Reaction 3)}$$

Reactions 1–3 show the mechanism in terms of catalytic Ni sites, although the same reaction is possible with the corresponding Co hydroxide and oxy(hydroxide). The catalytic regeneration of a stable metal hydroxide is supported by scanning electron microscopy and transmission electron microscopy images, which show no morphology changes after operations [16].

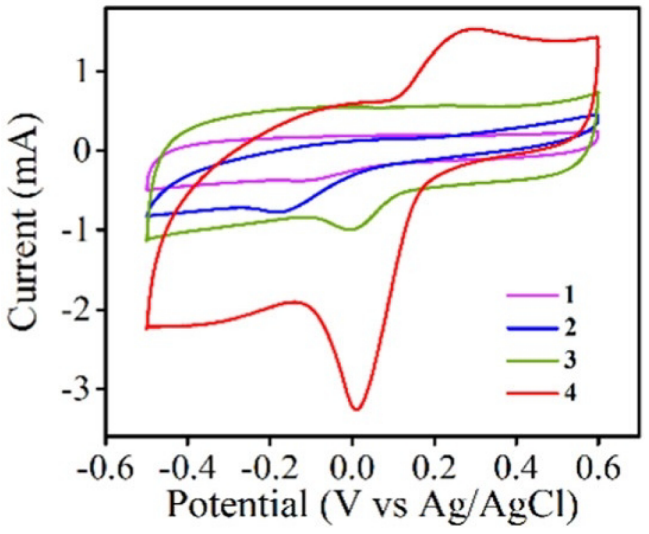

Fig. 3. Voltammetric responses acquired using a N-doped graphene/glassy carbon electrode (curve 1 and 2) and a nickel cobalt nitride/N-doped graphene/glassy carbon electrode (curve 3 and 4) in 0.1 M PBS without (curve 1 and 3) and with (curve 2 and 4) 1 mM H_2O_2 at 50 mV s^{-1}. This graph was obtained from [16] with the permission from ACS Publications.

Table 1 compares the voltammetric properties of the electrode materials reviewed in this paper for glucose oxidation. It is better to compare the onsets and peaks of glucose oxidation at the same scan rate as they might shift at different scan rates. Unfortunately, Xie and colleagues [19] did not record voltammetric responses at 50 mV s^{-1}.

2.2. Hydrogen peroxide (H_2O_2) sensors

H_2O_2 reduction has also been studied using several metal nitride materials. Based on our literature search, $NiCo_2N$ core shell nanohybrid on N-doped graphene electrodes developed by Deepalakshmi and co-workers [16] also exhibits the highest electrocatalytic activity towards hydrogen peroxide reduction amongst reported metal nitride electrodes. Here, the onset potentials for H_2O_2 reduction obtained using different metal nitride electrodes were compared in order to identify the best electrode material. The onset potential for the H_2O_2 reduction on a $NiCo_2N$ electrode is at around 0.3 V *vs.* Ag/AgCl and the reduction peak can be observed at approximately 0 V *vs.* Ag/AgCl as shown in Fig. 3.

The cyclic voltammogram recorded at $NiCo_2N$ in the absence of H_2O_2 does not exhibit an oxidation peak that can be ascribed to the $Ni^{2+/3+}$ and $Co^{2+/3+}$ redox processes, as was previously seen in the absence of glucose (Fig. 2). Nonetheless, a reduction peak is still seen in Fig. 3 at ~0 V *vs.* Ag/AgCl, which the authors assigned it to the reduction processes involving $Ni^{3+/2+}$ and $Co^{3+/2+}$. The absence of the oxidation peak for $Ni^{2+/3+}$ and $Co^{2+/3+}$ redox processes was not discussed by the authors [16]. It can also be observed that the reduction peak potential for $Ni^{3+/2+}$ and $Co^{3+/2}$ reactions in the absence of H_2O_2 (~0 V *vs.* Ag/AgCl; Fig. 3) is shifted to more negative values compared to that in the absence of glucose (~0.3 V *vs.* Ag/AgCl). This difference can likely be ascribed to a change in electrolyte (0.1 M NaOH for glucose, 0.1 M phosphate buffer solutions (PBS) for H_2O_2). Changes to the pH could impact the $Ni^{2+/3+}$ and $Co^{2+/3+}$ redox potential, or phosphate molecules may block the electrode surface hindering the redox processes of $Ni^{2+/3+}$ and $Co^{2+/3+}$, similar to the passivation of iron in phosphate solutions [22,23]. The electrode surface could have been reactivated when the potential is swept to more negative values, which enables the reduction peak to be observed on the cyclic voltammograms recorded in the absence of hydrogen peroxide.

The values for the sensitivity and the limit of detection for hydrogen peroxide reduction on $NiCo_2N$ electrodes are 2848.73 μA mM^{-1} cm^{-2} and 0.2 μM (S/N = 3) respectively. The linear ranges are found to be between 0.2 and 68.5 μM as well as from 198.5 to 3948.5 μM. Assuming the same key intermediates as for glucose oxidation, the mechanism could be expected to proceed via an initial electron transfer from catalytic metal sites to the hydrogen peroxide. The catalytic sites would then be recovered through charge transfer from the electrode.

$$Ni^{2+} + 2OH^- \rightleftharpoons Ni^{II}(OH)_2 \quad \text{(Reaction 4)}$$

$$Ni^{II}(OH)_2 + \frac{1}{2}H_2O_2 \rightleftharpoons Ni^{III}O(OH) + H_2O \quad \text{(Reaction 5)}$$

$$Ni^{III}O(OH) + H_2O + e^- \rightarrow Ni^{II}(OH)_2 + OH^- \quad \text{(Reaction 6)}$$

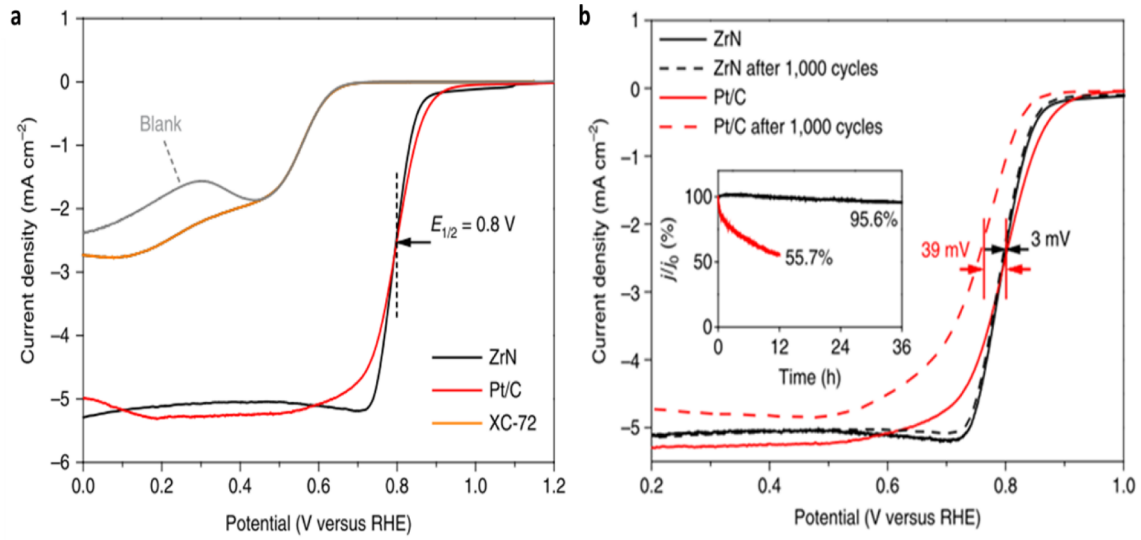

Fig. 4. (a) Linear sweep voltammograms of a ZrN/glassy carbon electrode, a Pt/C (XC-72 as the carbon support), a bare XC-72 electrode, and a bare glassy carbon electrode (blank) rotated at 1,600 r.p.m at the scan rate of 10 mV s^{-1} in O_2-saturated 0.1 M KOH solutions. The solutions were bubbled with O_2 gas for 30 mins. (b) Polarisation curves before (solid curves) and after (dashed curves) the accelerated durability tests. A graphite counter electrode was employed during the accelerated durability tests instead of a Pt wire to avoid the redeposition of Pt on the working electrode. The inset shows the chronoamperograms recorded during accelerated durability tests where the potential was fixed at a value which is not disclosed by Yuan et al. [25] but most probably at the diffusion-controlled region. These graphs were taken with permission from Springer Nature Limited [25].

However, as previously discussed, there is no evidence from the cyclic voltammetry that $Ni^{2+/3+}$ and $Co^{2+/3+}$ redox processes are occurring within the electrode material, so it is difficult to draw a solid conclusion. At this point, we strongly suggest that a further surface analysis to determine the oxidation states of the electrode materials must be performed. Deepalakshmi and co-workers [16] have characterised the surface after the material fabrication using an XPS. This revealed the chemical states of their sample surface, which include a few relevant core line spectra such as Ni 2p, C 1s, N 1s, and Co 2p.

Deepalakshmi and colleagues [16] mentioned that the intensity peaks of the Ni^{3+} state is higher than the Ni^{2+} state for the Ni 2p core line spectra. They speculated that this is due to the homogeneous doping of nitrogen, which may prevent a further surface oxidation process in the metal nitride species. However, there is a high possibility that their samples may undergo a surface oxidation process when they make contact with air or during voltammetric measurements. Van Bui and colleagues [24] mentioned that the surface of titanium nitride thin films may readily be oxidised to titanium oxynitride when exposed to air even at room temperature; this may also be the case for the metal nitride samples prepared by Deepalakshmi and colleagues [16]. Thus, Deepalakshmi and co-workers [16] should conduct XPS studies on their samples periodically.

Unfortunately, peaks that are attributed to oxygen can always be seen on most XPS spectra. Therefore, the authors should analyse the spectra carefully. One way to analyse the oxygen content in a sample is to observe the binding energy of other elements, in this case C 1s, O 1s, and Co 2p. The binding energy of these elements can be affected when surface oxidation occurs. The destruction of chemical states will lead to the shifting in the binding energy of these elements. Therefore, if the incorporation of nitrogen prevents the surface oxidation of their samples as claimed, there should not be a shift in the binding energy of these elements.

Deepalakshmi et al. [16] also stated that the presence of the core line spectrum of N 1s proved the incorporation of nitrogen into the electrode surface. However, we found that this statement needs more concrete evidence where they should collect Ni and Co 2p core line spectra before integrating nitrogen into the samples apart from presenting the XPS data after the incorporation of nitrogen. It is also necessary to conduct XPS studies for the graphene before and after decorating it with metal particles. Based on only the experimental data presented therein, it is difficult to make a solid conclusion on the oxidation states of Ni and Co in their samples.

The paper also did not show the effect of exposing the electrode material to either glucose or H_2O_2, which is highly important to show the stability of electrodes for continued electrochemical sensing. It is well understood that the products or by-products of glucose and H_2O_2 reduction may contaminate the electrode surface, but it is still possible to remove the contamination prior to conducting the XPS analysis. These additional data may enable researchers to make firm conclusions on the electrochemical processes and the oxidation states of Ni and Co in their samples.

2.3. Dissolved oxygen sensors

Recently, Yuan and colleagues [25] reported that zirconium nitride (ZrN) nanoparticles could be an alternative to platinum/carbon (Pt/C) electrodes for oxygen reduction reaction (ORR). This is a key research area given the urgent need to find a substitute for Pt, since noble metals are expensive. The ZrN nanoparticles were produced via an urea-glass route using zirconium chloride ($ZrCl_4$) as the metal source. In brief, ZrN powder was dispersed in ethanol. Subsequently, urea was added into the solution and the mixture was stirred. The solution was stored for 12 h before being heated in argon environment using a tubular furnace at 800 °C for 3 h. The ZrN nanoparticles were decorated on glassy carbon disk electrodes for ORR applications.

The onset potentials for the ORR obtained using ZrN and Pt/C electrodes are 0.89 V and 0.93 V *vs.* reversible hydrogen electrode (RHE) respectively (Fig. 4(a)). This means that the ZrN electrodes are more electrocatalytically active towards ORR than Pt/C. However, they both display the same value of half-wave potential ($E_{1/2}$) at 0.8 V *vs.* RHE. Yuan et al. [25] also demonstrated that the ZrN electrodes are more stable than the Pt/C electrodes for the ORR even after 1000 cycles as shown in Fig. 4(b). Importantly, the number of electrons transferred for the ORR at ZrN is four. This implies that oxygen is completely reduced to water with no observable two-electron reduction to H_2O_2, which is highly desirable for fuel cell applications. This is also

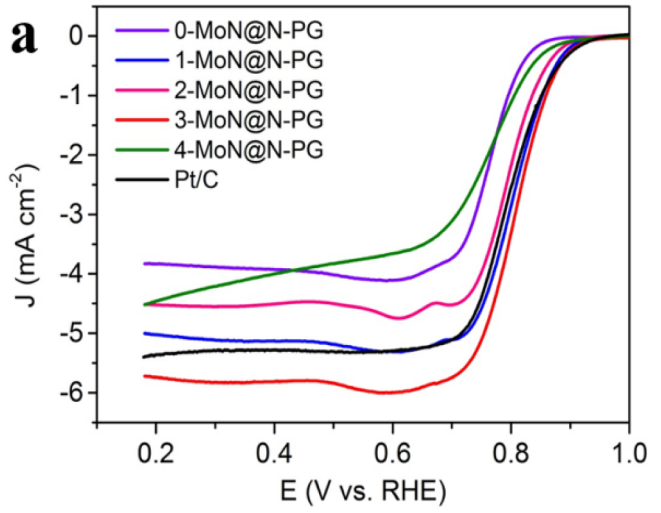

Fig. 5. ORR waves recorded using x-MoN/N-doped graphene electrodes (x = 0, 1, 2, 3, and 4) where x is the different amounts of H_2O_2 in mL used to prepare the MoN materials as well as commercial 20 wt% Pt/C catalysts at 5 mV s^{-1} at 1,600 r.p.m in O_2-saturated 0.1 M KOH solutions. Permission was obtained from Wiley VCH to display the graph from Liu et al. [27].

important for dissolved oxygen sensors, since the number of electrons must be well known to calculate a concentration from electrochemical data, and a larger charge per unit O_2 will give a lower limit of detection [26].

Liu and colleagues [27] investigated molybdenum nitride (MoN) on N-doped graphene as an alternative ORR catalyst. They reported that the electrocatalytic current for the ORR at one of their MoN electrodes (3-MoN@N-PG) is higher than that recorded with Pt/C (Fig. 5). However, recorded currents are also determined by the electrode area and the catalytst loading, so it is not recommended to compare the currents acquired using different materials without adequate normalisation by geometry or mass loading. Additionally, the onset potential for the ORR acquired by their MoN electrodes is more positive (0.93 V *vs.* RHE) than that recorded using the ZrN electrodes (0.89 V *vs.* RHE). This suggests that MoN at N-doped graphene may be the superior ORR catalyst, although only a 40 mV difference in overpotential should not rule out either material. Table 2 summarises the voltammetric features determined using the electrode materials reviewed in this article for easier comparison. The next section introduces MoN solid microdisk electrodes.

2.4. Advancement for metal nitride materials as electrosensors

For this section, MoN microdisk electrodes prepared by Shafiee et al. [28] were chosen because their electrodes are easy to fabricate, robust, and convenient since they just need to be polished to gain a fresh electrode surface. Shafiee et al. [28] fabricated solid molybdenum nitride microdisk electrodes from MoN wires. The wires were first prepared via nitridation process from commercially available 25 μm diameter Mo wires, which were cut into small pieces. Most of the metal nitride electrodes prepared by other groups were in the form of either thin films or powders [16,25]. Unfortunately, thin films have the tendency to blister, delaminate, or form cracks during sample preparation or usage [29]. This exposes the underlying substrate and increases the surface area, which introduces significant error into electrochemical sensing data. Their solid molybdenum nitride microdisk electrodes address this problem, and exhibit a diffusion-controlled cyclic voltammogram for the reduction of peroxodisulphate at a slow scan rate (Fig. 6(a)), which has never been achieved with other bare electrodes [30–33]. The presence of N atoms in the metal may have a role in making the peroxodisulphate reduction diffusion-controlled. It is also possible that the act of polishing the electrode surface activated the MoN surface; the activation of solid MoN by mechanical polishing could be akin to that of Pt electrode surface as reported by Lee and colleagues [34]. It would be interesting to use solid MoN microdisk electrodes to investigate other complicated redox processes. Unfortunately, the upper potential limit for this electrode is ~0.3 V *vs.* saturated calomel electrode (SCE), i.e. where oxygen evolution reaction starts to occur (Fig. 6(b)). Nevertheless, this shows that solid MoN microdisk electrodes could be used to probe other species where the redox potentials are within this potential window.

3. Conclusion

Metal nitride materials are promising candidates for electrochemical applications thanks to their high conductivity, thermal stability, hardness and corrosion resistance [35]. Incorporating nanoparticulate metal nitrides into active supports such as 3D N-doped carbons, metallic meshes or hybrid metal nitrides enhances electron transfer, facilitates product and react diffusion and exposes additional catalytic sites, providing further improvements to their electrochemical performance [36]. Newly developed materials often focus on bimetallic nitrides, which tend to outperform their component nitride by optimising reactant binding to the catalyst surface, or through the synergistic activity of neighbouring metal sites [37,38].

The origin of their catalytic activity has been proposed to be the *in situ* formation of metal oxides and oxy(hydroxide), which give high oxidation state metal sites. The fact that these are generated *in situ* results in a thin film oxide/oxy(hydroxide) film on a metal nitride core, which facilitates charge transfer from/to the material and favours overall catalyst stability by hindering overall dissolution of the catalysts [21].

$NiCo_2N$ electrodes seemed to be the best sensor for both glucose and H_2O_2. Meanwhile, ZrN or MoN materials could replace Pt/C for ORR. This interesting finding has offered a new candidate for dissolved oxygen sensors. It is possible to fabricate solid metal nitride electrodes that can be mechanically polished, which could enhance the electrochemical responses for complicated electrochemical reactions. Metal nitride materials have applications for various fields, especially as electrochemical sensors. Further efforts are needed to explore the full potential of metal nitride electrodes.

Declaration of Competing Interest

The authors declare that they have no known competing financial interests or personal relationships that could have appeared to influence the work reported in this paper.

Table 2
An overview of the voltammetric features and experimental conditions for the ORR for ZrN nanoparticles and MoN N-doped graphene. NP is an abbreviation for nanoparticles.

Electrode material	Onset/V *vs.* RHE	Peak/V *vs.* RHE	Scan rate/mV s^{-1}	Solution	Apparent number of electrons transferred	Ref.
ZrN NP	0.89	0.7	10	O_2 saturated 0.1 M KOH	4	[25]
MoN N-doped graphene	0.93	0.7	5	O_2 saturated 0.1 M KOH	4	[27]

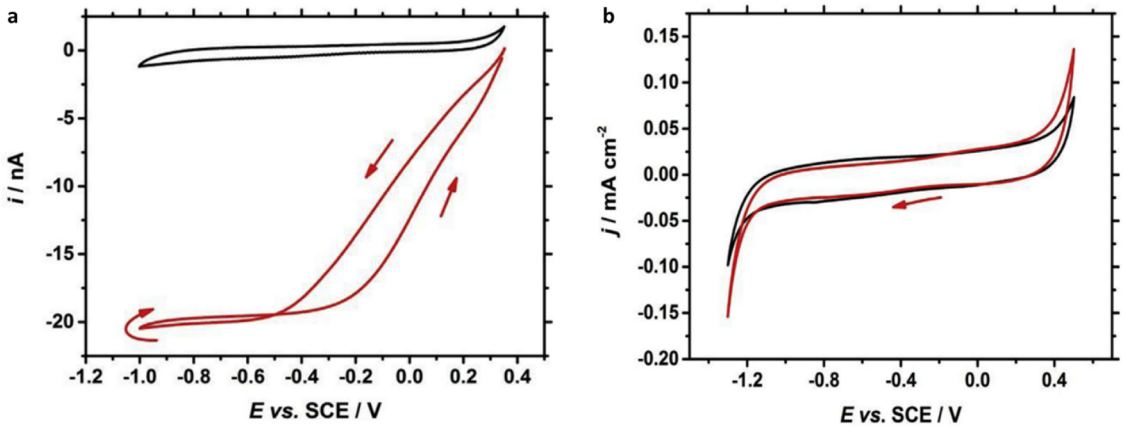

Fig. 6. (a) Cyclic voltammograms recorded using a 26 μm Ø solid MoN microdisk electrode in a deoxygenated 0.1 M $KClO_4$ solution in the presence (red) and in the absence (black) of 2 mM $K_2S_2O_8$ at 10 mV s^{-1}. (b) Voltammetric responses acquired using a 27 μm (black) and a 28 μm (red) Ø MoN microdisk electrodes in a deaerated 0.5 M KCl solution. These graphs were taken from Shafiee and co-workers [28] with the permission from Elsevier. (For interpretation of the references to colour in this figure legend, the reader is referred to the web version of this article.)

Acknowledgement

The authors would like to thank the publisher for waiving the publication fee.

Conflicts of interest

There are no conflicts of interest to declare.

References

[1] Y. Yuan, L. Yang, B. He, E. Pervaiz, Z. Shao, M. Yang, Cobalt-zinc nitride on nitrogen doped carbon black nanohybrids as a non-noble metal electrocatalyst for oxygen reduction reaction, Nanoscale 9 (2017) 6259–6263, https://doi.org/10.1039/c7nr02264f.

[2] X. Wang, W.T. Zheng, H.W. Tian, S.S. Yu, W. Xu, S.H. Meng, X.D. He, J.C. Han, C.Q. Sun, B.K. Tay, Growth, structural, and magnetic properties of iron nitride thin films deposited by DC magnetron sputtering, Appl. Surf. Sci. 220 (2003) 30–39, https://doi.org/10.1016/S0169-4332(03)00752-9.

[3] G.V. Chertihin, L. Andrews, M. Neurock, Reactions of laser-ablated iron atoms with nitrogen atoms and molecules. Matrix infrared spectra and density functional calculations of novel iron nitride molecules, J. Phys. Chem. 100 (1996) 14609–14617, https://doi.org/10.1021/jp961423j.

[4] U. Rajaji, A. Muthumariyappan, S.M. Chen, T.W. Chen, R.J. Ramalingam, A novel electrochemical sensor for the detection of oxidative stress and cancer biomarker (4-nitroquinoline N-oxide) based on iron nitride nanoparticles with multilayer reduced graphene nanosheets modified electrode, Sens. Actuators B Chem. 291 (2019) 120–129, https://doi.org/10.1016/j.snb.2019.04.041.

[5] S. Dutta, A. Indra, Y. Feng, H.S. Han, T. Song, Promoting electrocatalytic overall water splitting with nanohybrid of transition metal nitride-oxynitride, Appl. Catal. B Environ. 241 (2019) 521–527, https://doi.org/10.1016/j.apcatb.2018.09.061.

[6] M. Zheng, X. Chen, R. Cheng, N. Li, J. Sun, X. Wang, T. Zhang, Catalytic decomposition of hydrazine on iron nitride catalysts, Catal. Commun. 7 (2006) 187–191, https://doi.org/10.1016/j.catcom.2005.10.009.

[7] M. Jiang, Y. Li, Z. Lu, X. Sun, X. Duan, Binary nickel-iron nitride nanoarrays as bifunctional electrocatalysts for overall water splitting, Inorg. Chem. Front. 3 (2016) 630–634, https://doi.org/10.1039/c5qi00232j.

[8] Y. Wang, C. Xie, D. Liu, X. Huang, J. Huo, S. Wang, Nanoparticle-stacked porous nickel-iron nitride nanosheet: a highly efficient bifunctional electrocatalyst for overall water splitting, ACS Appl. Mater. Interfaces 8 (2016) 18652–18657, https://doi.org/10.1021/acsami.6b05811.

[9] S.A. Rasaki, B. Zhang, K. Anbalgam, T. Thomas, M. Yang, Synthesis and application of nano-structured metal nitrides and carbides: a review, Prog. Solid State Chem. 50 (2018) 1–15, https://doi.org/10.1016/j.progsolidstchem.2018.05.001.

[10] L. Chen, J. Song, Tailored graphitic carbon nitride nanostructures: synthesis, modification, and sensing applications, Adv. Funct. Mater. 27 (2017) 1702695, https://doi.org/10.1002/adfm.201702695.

[11] A. Wang, C. Wang, L. Fu, W. Wong-Ng, Y. Lan, Recent advances of graphitic carbon nitride-based structures and applications in catalyst, sensing, imaging, and LEDs, Nano-Micro Lett. 9 (2017) 1–21, https://doi.org/10.1007/s40820-017-0148-2.

[12] F. Magesa, Y. Wu, Y. Tian, J.M. Vianney, J. Buza, Q. He, Y. Tan, Graphene and graphene like 2D graphitic carbon nitride: electrochemical detection of food colorants and toxic substances in environment, Trends Environ. Anal. Chem. 23 (2019) e00064, , https://doi.org/10.1016/j.teac.2019.e00064.

[13] M.M. Xavier, P.R. Nair, S. Mathew, Emerging trends in sensors based on carbon nitride materials, Analyst 144 (2019) 1475–1491, https://doi.org/10.1039/c8an02110d.

[14] D.W. Hwang, S. Lee, M. Seo, T.D. Chung, Recent advances in electrochemical non-enzymatic glucose sensors – a review, Anal. Chim. Acta 1033 (2018) 1–34, https://doi.org/10.1016/j.aca.2018.05.051.

[15] K. Dhara, D.R. Mahapatra, Electrochemical nonenzymatic sensing of glucose using advanced nanomaterials, Microchim. Acta 185 (2018) 49, https://doi.org/10.1007/s00604-017-2609-1.

[16] T. Deepalakshmi, D.T. Tran, N.H. Kim, K.T. Chong, J.H. Lee, Nitrogen-doped graphene-encapsulated nickel cobalt nitride as a highly sensitive and selective electrode for glucose and hydrogen peroxide sensing applications, ACS Appl. Mater. Interfaces 10 (2018) 35847–35858, https://doi.org/10.1021/acsami.8b15069.

[17] R. Ramli, A.Z. Omar Arawi, M.M. Mahat, A. Faiza Mohd., M.F.Z.R. Yahya, Effect of silver (Ag) substitution nano-hydroxyapatite synthesis by microwave processing, in: ICBEIA 2011 – 2011 Int. Conf. Business, Eng. Ind. Appl., 2011. pp. 180–183. Doi:10.1109/ICBEIA.2011.5994237.

[18] J. Chen, H. Yin, J. Zhou, J. Gong, L. Wang, Y. Zheng, Q. Nie, Non-enzymatic glucose sensor based on nickel nitride decorated nitrogen doped carbon spheres (Ni_3N/NCS) via facile one pot nitridation process, J. Alloys Compd. 797 (2019) 922–930, https://doi.org/10.1016/j.jallcom.2019.05.234.

[19] F. Xie, T. Liu, L. Xie, X. Sun, Y. Luo, Metallic nickel nitride nanosheet: an efficient catalyst electrode for sensitive and selective non-enzymatic glucose sensing, Sens. Actuators B Chem. 255 (2018) 2794–2799, https://doi.org/10.1016/j.snb.2017.09.095.

[20] X. Dai, W. Deng, C. You, Z. Shen, X. Xiong, X. Sun, A Ni_3N-Co_3N hybrid nanowire array electrode for high-performance nonenzymatic glucose detection, Anal. Methods 10 (2018) 1680–1684, https://doi.org/10.1039/c8ay00370j.

[21] L. Yu, Q. Zhu, S. Song, B. McElhenny, D. Wang, C. Wu, Z. Qin, J. Bao, Y. Yu, S. Chen, Z. Ren, Non-noble metal-nitride based electrocatalysts for high-performance alkaline seawater electrolysis, Nat. Commun. 10 (2019) 5106, https://doi.org/10.1038/s41467-019-13092-7.

[22] J. Benzakour, A. Derja, Characterisation of the passive film on iron in phosphate medium by voltammetry and XPS measurements, J. Electroanal. Chem. 437 (1997) 119–124, https://doi.org/10.1016/S0022-0728(97)00337-9.

[23] K. Azumi, T. Ohtsuka, N. Sato, Impedance of iron electrode passivated in borate and phosphate solutions, Trans. Japan Inst. Met. 27 (1986) 382–392, https://doi.org/10.2320/matertrans1960.27.382.

[24] H. Van Bui, A.W. Groenland, A.A.I. Aarnink, R.A.M. Wolters, J. Schmitz, A.Y. Kovalgin, Growth kinetics and oxidation mechanism of ALD TiN thin films monitored by in situ spectroscopic ellipsometry, J. Electrochem. Soc. 158 (2011) H214, https://doi.org/10.1149/1.3530090.

[25] Y. Yuan, J. Wang, S. Adimi, H. Shen, T. Thomas, R. Ma, J.P. Attfield, M. Yang, Zirconium nitride catalysts surpass platinum for oxygen reduction, Nat. Mater. 19 (2019) 282–286, https://doi.org/10.1038/s41563-019-0535-9.

[26] S.C. Perry, G. Denuault, Transient study of the oxygen reduction reaction on reduced Pt and Pt alloys microelectrodes: evidence for the reduction of pre-adsorbed oxygen species linked to dissolved oxygen, Phys. Chem. Chem. Phys. 17 (2015) 30005–30012, https://doi.org/10.1039/c5cp04667j.

[27] X. Liu, I.S. Amiinu, S. Liu, Z. Pu, W. Li, B. Ye, D. Tan, S. Mu, H_2O_2-assisted synthesis of porous N-doped graphene/molybdenum nitride composites with boosted oxygen reduction reaction, Adv. Mater. Interfaces 4 (2017) 1601227, https://doi.org/10.1002/admi.201601227.

[28] S.A. Bin Shafiee, A.L. Hector, G. Denuault, Solid molybdenum nitride microdisc electrodes: fabrication, characterisation, and application to the reduction of peroxodisulfate, Electrochim. Acta 293 (2018) 184–190, https://doi.org/10.1016/j.electacta.2018.10.046.

[29] M.J. Kim, Molybdenum nitride film formation, J. Electrochem. Soc. 130 (1983) 1196, https://doi.org/10.1149/1.2119916.

[30] G.N. Botukhova, O.A. Petrii, Electroreduction of peroxodisulfate anion at platinum rotating disc electrode in the cyclic voltammetry mode, Russ. J. Electrochem. 49 (2012) 1145–1153, https://doi.org/10.1134/s1023193512090042.
[31] Z. Samec, K. Doblhofer, Mechanism of peroxodisulfate reduction at a polycrystalline gold electrode, J. Electroanal. Chem. 367 (1994) 141–147, https://doi.org/10.1016/0022-0728(93)03041-M.
[32] Z. Samec, A.M. Bittner, K. Doblhofer, Electrocatalytic reduction of peroxodisulfate anion on Au(111) in acidic aqueous solutions, J. Electroanal. Chem. 409 (1996) 165–173, https://doi.org/10.1016/0022-0728(95)04411-6.
[33] S.A. Shafiee, J. Aarons, H.H. Hamzah, Review—electroreduction of peroxodisulfate: a review of a complicated reaction, J. Electrochem. Soc. (2018), https://doi.org/10.1149/2.1161811jes.
[34] J. Lee, D.W.M. Arrigan, D.S. Silvester, Mechanical polishing as an improved surface treatment for platinum screen-printed electrodes, Sens. Bio-Sens. Res. 9 (2016) 38–44, https://doi.org/10.1016/j.sbsr.2016.05.006.
[35] X. Tian, J. Luo, H. Nan, Z. Fu, J. Zeng, S. Liao, Binary transition metal nitrides with enhanced activity and durability for the oxygen reduction reaction, J. Mater. Chem. A 3 (2015) 16801–16809, https://doi.org/10.1039/c5ta04410c.
[36] A.K. Tareen, G.S. Priyanga, K. Khan, E. Pervaiz, T. Thomas, M. Yang, Nickel-based transition metal nitride electrocatalysts for the oxygen evolution reaction, ChemSusChem 12 (2019) 3941–3954, https://doi.org/10.1002/cssc.201900553.
[37] Y. Wang, Y. Sun, F. Yan, C. Zhu, P. Gao, X. Zhang, Y. Chen, Self-supported NiMo-based nanowire arrays as bifunctional electrocatalysts for full water splitting, J. Mater. Chem. A 6 (2018) 8479–8487, https://doi.org/10.1039/c8ta00517f.
[38] S. Sultan, J.N. Tiwari, J.-H. Jang, A.M. Harzandi, F. Salehnia, S.J. Yoo, K.S. Kim, Highly efficient oxygen reduction reaction activity of graphitic tube encapsulating nitrided Co_xFe_y alloy, Adv. Energy Mater. 8 (2018) 1801002, https://doi.org/10.1002/aenm.201801002.